**Response to reviewers**

**Reviewer 1**

Line 349-352: STSW was defined using the 15 C isotherm as a cut-off. That is all data ≥15 C were grouped as STSW. The depth of this isotherm varied by station but with a mean depth of 144 ± 96 m for the three transects. For SASW, in order to compare most effectively with STSW we used the mean depth of 15 C. So effectively, STSW was defined by 15 C and SASW by the mean depth of 15 C in STSW. For clarity, on lines 349-353 we have now made clear the 15 C isotherm was used to define STSW on a station by station basis but for SASW the mean depth of 15C was used.

Line 353: We used an average inventory over set depths, either defined by 15 C (STSW) or the mean depth of 15 C (SASW). This means that the removal of certain data points due to continental input would not significantly affect the inventories.

Line 363: Yes, these are concentration inventory ratios. We first introduce these ratios on line 358 and make it clear we are referring to concentration inventory ratios. We have now also made this explicitly clear in the table 2 caption.

Line 401: We have now included the term 'inventory ratio' throughout the text for clarity.

Line 450 Indeed Cd could play a role and support cellular function under low Zn conditions. Unfortunately, we do not have a complete Cd data set with which to assess such assumption. Instead, we make reference to the fact Cd can also play a role in carbonic anhydrase and cambialistic metabolism on lines 55, 439, 442, 458 and 530.

Line 500: Agreed, we have now completed this sentence to read 'Conversely, the absence of a significant diatom contribution to summer SASW chlorophyll-a (Fig. 5a), relative to early spring, is surprising as the summer dZn/PO43- inventory ratio is in excess of the cellular Zn/P requirements of typical oceanic diatoms such as T. oceanica (Fig. 6).'

Line 504: We have now clarified that T oceanica have been shown to grow effectively at low Co concentration in the presence of Zn.

Lines 504-510 We have tried to express NO3 vs Si as published elsewhere i.e. NO3/Si ratios. We have also reported the absolute concentrations alongside these ratios, as per table 2 for metals vs P, to aid the reader.

**Reviewer 2**

Lines 126 & 131: We do not use the lowest standard deviation per say, but rather the standard deviation from the lowest concentration standard during the analytical run. The error associated with such low concentrations is typically larger than that of higher concentrations. Second, we have taken the mean detection limit from combined analytical runs as the value we report here. To clarify this, we have changed the term 'lowest standard addition' to 'lowest concentration standard' and have now included the number of analytical runs the over that the detection limit was calculated.

Line 286-297: We feel that 7 ½ lines is not too lengthy to make the point dust deposition is minimally affecting mixed layer Zn and Co inventories. Previously I have been asked to provide better explanation of the deposition calculations and I have tried to condense this as much as possible.

Line 313: We have however shortened the riverine section slightly on the request of reviewer 2.

# Seasonal cycling of zinc and cobalt in the Southeast Atlantic along the GEOTRACES GA10 section.

Neil J. Wyatt[1], Angela Milne[2], Eric P. Achterberg[3], Thomas J. Browning[3], Heather A. Bouman[4], E. Malcolm S. Woodward[5], Maeve C. Lohan[1].

[1]Ocean and Earth Science, National Oceanography Centre, University of Southampton, Southampton, United Kingdom.

[2]School of Geography, Earth and Environmental Sciences, University of Plymouth, Plymouth, United Kingdom.

[3]Marine Biogeochemistry Division, GEOMAR Helmholtz Centre for Ocean Research, Kiel, Germany.

[4]Department of Earth Sciences, University of Oxford, Oxford, United Kingdom.

[5]Plymouth Marine Laboratory, Plymouth, United Kingdom.

Correspondence to: N. J. Wyatt (n.j.wyatt@soton.ac.uk)

**Abstract**

We report the distributions and stoichiometry of dissolved zinc (dZn) and cobalt (dCo) in sub-tropical and sub-Antarctic waters of the Southeast Atlantic Ocean during austral spring 2010 and summer 2011/12. In sub-tropical surface waters, mixed-layer dZn and dCo concentrations during early spring were 1.60 ± 2.58 nM and 30 ± 11 pM, respectively, compared with summer values of 0.14 ± 0.08 nM and 24 ± 6 pM. The elevated spring dZn concentrations resulted from an apparent offshore transport of elevated dZn at depths between 20 – 55 m, derived from from the Agulhas Bank. In contrast, open-ocean sub-Antarctic surface waters displayed largely

consistent inter-seasonal mixed-layer dZn and dCo concentrations of 0.10 ± 0.07 nM and 11 ± 5 pM, respectively. Trace metal stoichiometry, calculated from concentration inventories, suggest a greater overall removal for dZn relative to dCo in the upper water column of the Southeast Atlantic with an inter-seasonally decreasing dZn/dCo inventory ratios of 19 to 5 mol $mol^{-1}$ and 13 to 7 mol $mol^{-1}$ for sub-tropical surface water and sub-Antarctic surface water, respectively. In this paper, we investigate how the seasonal influences of external input and phytoplankton succession may relate to the distribution of dZn and dCo, and variation in dZn/dCo stoichiometry, across these two distinct ecological regimes in the Southeast Atlantic.

## 1. Introduction

The trace metal micronutrients zinc (Zn) and cobalt (Co) play an important role in the productivity of the oceans as key requirements in marine phytoplankton metabolism (Morel, 2008; Twining and Baines, 2013). Zinc is required for the acquisition of inorganic carbon and organic phosphorus via the carbonic anhydrase and alkaline phosphatase metalloenzymes, respectively (Morel et al., 1994; Shaked et al., 2006; Cox and Saito, 2013). The requirement for Co stems from its obligation in the biosynthesis of vitamin $B_{12}$ (Raux et al., 2000; Rodionov et al., 2003) and, like Zn, its potential roles as a metal cofactor in carbonic anhydrase and alkaline phosphatase (Morel et al., 1994; Jakuba et al., 2008; Saito et al., 2017). Significantly, both dissolved Zn (dZn) and Co (dCo) are often scarce in surface seawater with mean concentrations that are often similar to, or relatively depleted, compared with typical cellular requirements of phytoplankton (Moore et al., 2013; Moore, 2016). Hence, dZn and dCo availability have the potential to regulate phytoplankton metabolism and growth rates in some ocean regions (Sunda and Huntsman, 1992; Saito et al., 2002; Franck et al., 2003; Shaked et al., 2006; Bertrand et al., 2007; Jakuba et al., 2012; Mahaffey et al., 2014; Chappell et al., 2016; Browning et al., 2017).

The role for Zn and Co in carbonic anhydrase establishes an interaction between their ocean cycles, whereby biochemical substitutions between the enzyme-bound metals enables a stoichiometric plasticity in their cellular requirements that can negate the effect of limited availability. For example, a number of eukaryotic algae can substitute Zn for Co, as well as cadmium (Cd), in carbonic anhydrase when seawater dZn concentrations are low (Price and Morel, 1990; Sunda and Huntsman, 1995; Lane and Morel, 2000; Xu et al., 2007; Saito and Goepfert, 2008; Kellogg et al., 2020). In contrast, the prokaryotic picocyanobacteria *Synechococcus* and *Prochlorococcus* appear to have an absolute Co requirement (Sunda and Huntsman, 1995; Saito et al., 2002; Hawco and Saito, 2018). The availability and stoichiometry of dZn and dCo may therefore also exert a key control on phytoplankton community structure in some ocean regions (Leblanc et al., 2005; Saito et al., 2010; Chappell et al., 2016).

With the arrival of GEOTRACES research cruises, a number of studies have provided comprehensive data on the basin-scale distributions of Zn and Co in the Atlantic Ocean (e.g. Bown et al., 2011; Noble et al., 2012, 2017; Wyatt et al., 2014; Roshan et al., 2015; Middag et al., 2018). Such efforts have transformed our understanding of the biogeochemical processes associated with Zn and Co cycling (Saito et al., 2017; Vance et al., 2017; Weber et al., 2018; Tagliabue et al., 2018; Roshan et al., 2018) yet there are still geographically important regions of the Atlantic that remain largely understudied, including the Southeast Atlantic.

The Sub-Tropical Front (STF) of the Southeast Atlantic represents the convergence of warm, predominately macronutrient-limited Sub-Tropical Surface Water (STSW) and cold, iron-limited but macronutrient enriched sub-Antarctic Surface Water (SASW), creating one of the most dynamic nutrient regimes in the oceans (Ito et al., 2005; Browning et al., 2014; Moore, 2016). Here, the relative supply and availability of macronutrients and iron (Fe) exert an important control in maintaining the elevated phytoplankton stock and productivity that is typical of this frontal region, particularly during austral spring and summer (Moore and Abbott,

2000; Ito et al., 2005; Browning et al., 2014). Dissolved Zn is also depleted in SASW that flows northwards to converge with STSW at the STF (Wyatt et al., 2014). However, the potential role for Zn in the mediation of phytoplankton distribution and community structure in this region is currently unclear.

Using data from two UK-GEOTRACES cruises (transect GA10) this study examines the seasonal availability and ecological stoichiometry of dZn and dCo, by analysis of their relationships with phosphate, in upper ocean waters of the Southeast Atlantic. These data, together with measurements of phytoplankton pigment biomass and community structure, offer an improved knowledge of the seasonal influences of external input and phytoplankton succession on the distribution and cycling of Zn and Co in these dynamic waters.

## 2. Methods

### 2.1. Sampling methods

Seawater samples were collected during two UK-GEOTRACES cruises in the South Atlantic Ocean (GA10, Fig. 1). The first cruise (D357) took place during austral spring 2010 (18th October to 22nd November 2010), sampling the Southeast Atlantic on-board the *RSS Discovery*. During D357, two transects were completed between Cape Town and the zero meridian that represent early austral spring (D357-1) and late austral spring (D357-2), respectively. The second cruise (JC068) took place during austral summer 2011/2012 (24th December 2011 to 27th January 2012), along the same transect of the first cruise and continuing along 40ºS between Cape Town and Montevideo, Uruguay, on-board the *RSS James Cook*. For JC068, we present here only the repeat transect data between Cape Town and 13°W that represents the Southeast Atlantic aspect of this transect. The stations occupied during the three transects were not identical, but rather represent a coverage of the Southern Ocean and sub-

tropical waters present. Where stations were reoccupied during one or more transects, they have the same station number.

All sampling bottles were cleaned according to the procedures detailed in the GEOTRACES sample handling protocols (Cutter et al., 2010). Seawater and particulate samples below 15 m depth were collected using a titanium-frame CTD with 24 trace metal clean 10 L Teflon-coated OTE (Ocean Test Equipment) Niskin bottles deployed on a plasma rope. Sub-samples for dissolved trace metal analysis were filtered through 0.8/0.2 µm cartridge filters (AcroPak™ 500, Pall) into 125 mL low density polyethylene bottles inside a class 1000 clean air container. Each sub-sample was acidified to pH 1.7 (0.024 M) by addition of 12 M hydrochloric acid (HCl, UpA, Romil) under a class 100 laminar flow hood. Vertical sampling for dissolved trace metals was augmented by surface samples collected at each station using a towed 'fish' positioned at approximately 3-5 m depth. Fish samples were filtered in-line and acidified as described for samples collected from the titanium sampling system. Particulate samples were collected onto acid clean 25 mm, 0.45 µm, polyethersulfone membrane disc filters (Supor®, Pall) and stored frozen (-20ºC) until shore-based analysis.

### 2.2. Trace metal analysis

Dissolved Co was determined in the ISO accredited clean room facility (ISO 9001) at the University of Plymouth (UK) using flow injection with chemiluminescence detection, modified from the method of Cannizzaro et al. (1999) as described by Shelley et al. (2010). Briefly, dCo was determined in UV-irradiated samples using the reaction between pyrogallol (1,2,3-trihydrobenzene) and hydrogen peroxide formed in the presence of Co. Standards (20 – 120 pM Co) were prepared in 0.2 µm filtered low-dCo seawater (16.5 ± 5.2 pM, $n$ = 15) by serial dilution of a 1000 ppm Co ICP-MS standard (Romil, UK). The accuracy of the analytical method was validated by quantification of dCo in SAFe (S and D2) and GEOTRACES (GD)

reference seawater (Table 1). There was no detectable analytical dCo blank and the limit of detection (3σ of the lowest concentration standard) was 1.98 ± 0.87 pM ($n$ = 15). Dissolved Zn was determined using flow injection coupled with fluorescence detection, modified from the method of Nowicki et al. (1994) and described previously for this GEOTRACES section by Wyatt et al. (2014). The accuracy of the analytical method was validated by quantification of dZn in SAFe (S and D2) reference seawater (Table 1). The blank for dZn FIA was 0.14 ± 0.13 nM and the limit of detection (3σ of the lowest concentration standard) was 0.01 ± 0.01 nM ($n$ = 15).

**Commented [NW1]:** Reviewer 2 comment: We have now clarified that the detection limit is calculate from the lowest concentration standard over 15 analytical runs.

**Commented [NW2]:** Reviewer 2 comment: We have now clarified that the detection limit is calculate from the lowest concentration standard over 15 analytical runs.

Measurement uncertainties were estimated after the Nordtest approach (Worsfold et al., 2019) where a combined uncertainty ($u_c$) is computed from day-to-day within-lab reproducibility and uncertainties associated with the determination of reference materials (Table 1). This approach creates higher uncertainties than those previously published for dZn and dCo analyses but provides a more realistic estimation of analytical uncertainty. During this study, the $u_c$ for dZn and dCo analysis was 22 and 19 %, respectively, similar to the 13 – 25 % reported by Rapp et al. (2017) for the determination of trace metals, including dZn and dCo, by on-line pre-concentration and high-resolution sector field ICP-MS detection. The elevated $u_c$ within our data results from the greater uncertainty surrounding the very low dZn and dCo concentration SAFe S reference sample whereas the dZn and dCo $u_c$ using only the Safe D2 are <5 %. Hereafter, when presenting low dZn and dCo concentrations for comparison with phytoplankton biological requirements (Section 3.5), we apply a fixed $u_c$ of 20 % to our data.

Total particulate trace metals (i.e. pZn, pCo, pTi) were determined using inductively coupled plasma-mass spectrometry (Thermo Fisher XSeries-2) following a sequential acid digestion modified from Ohnemus et al. (2014). Potential interferences (e.g. $_{40}Ar_{16}O$ on $_{56}Fe$) were minimized through the use of a collision/reaction cell utilizing 7 % H in He and evaluation of

efficiency and accuracy assessed using Certified Reference Material (CRM). Full details of the method and CRM results can be found in Milne et al. (2017).

### 2.3. Nutrients, phytoplankton, temperature and salinity

The dissolved macronutrients phosphate ($PO_4^{3-}$), silicic acid ($Si(OH)_4$ but referred to as Si hereafter) and nitrate (determined as nitrate + nitrite, $NO_3^-$) were determined in all samples for which trace metals were determined, in addition to samples collected from a stainless steel rosette. Macronutrients were determined using an AA III segmented-flow AutoAnalyzer (Bran & Luebbe) following colorimetric procedures (Woodward and Rees, 2001). Salinity, temperature and depth were measured using a CTD system (Seabird 911+) whilst dissolved $O_2$ was determined using a Seabird SBE 43 $O_2$ sensor. Salinity was calibrated on-board using discrete samples taken from the OTE bottles and an Autosal 8400B salinometer (Guildline) whilst dissolved $O_2$ was calibrated using a photometric automated Winkler titration system (Carritt and Carpenter, 1966). Mixed-layer depths (MLD) were calculated using the threshold method of de Boyer Montégut et al. (2014), where MLD is identified from a linear interpolation between near-surface density and the depth at which density changes by a threshold value (0.125 kg $m^{-3}$).

Measurements of phytoplankton pigment biomass and community structure were made on discrete samples collected using a 24 position stainless-steel CTD rosette equipped with 20 L OTE Niskin bottles. For chlorophyll-*a* analysis, samples were filtered (0.7 µm Whatman GF/F) and then the filters extracted overnight in 90 % acetone (Holm-Hansen et al., 1965). The chlorophyll-*a* extract was measured on a pre-calibrated (spinach chlorophyll-*a* standard, Sigma) Turner Designs Trilogy fluorometer. High performance liquid chromatography (HPLC) samples (0.5 – 2 L) for accessory pigment analyses were filtered (0.7 µm Whatman GF/F), flash frozen in liquid nitrogen and stored at -80 °C prior to analysis using a Thermo

HPLC system. The matrix factorization program CHEMTAX was used to estimate the contribution of taxonomic groups to total chlorophyll-*a* (Mackey et al., 1996). Concentrations of nanophytoplankton, *Synechococcus*, *Prochlorococcus* and photosynthetic picoeukaryotes were analysed by analytical flow cytometry (AFC) using a FACSort flow cytometer (Becton Dickenson, Oxford, UK) according to the methods described in Davey et al. (2008) and Zubkov et al. (2003).

## 3. Results and Discussion

### 3.1. Hydrographic setting and macronutrient distributions

The prominent waters masses along the D357 and JC068 transects (Fig. 2) were identified by their characteristic thermohaline and macronutrient properties (Sarmiento et al., 2004; Ansorge et al., 2005; Browning et al., 2014). Wyatt et al. (2014) provide a more detailed description of the JC068 hydrography along the entire GA10 section. Whilst we aim to compare the nearshore versus offshore distributions of micro- and macronutrients, note that sub-Antarctic mode water was not sampled for trace metals during the D357-2 late spring transect, and therefore only the early spring and summer values are discussed for SASW hereafter.

***Surface mixed-layer***

During all three transects the STF was identified by a sharp potential temperature ($\theta$) gradient in the upper 200 m with the $\theta$ 15°C isotherm corresponding well to changes in macronutrient concentrations between STSW and SASW. North of the STF, mixed-layer macronutrient concentrations (Table 2) decreased in STSW between the three occupations of the transect. The largest relative depletion observed was for $NO_3^-$ with a ~2.7-fold reduction in mean inventory concentration from 870 to 326 µmol $m^{-3}$ between early spring and summer, whilst $PO_4^{3-}$ and Si concentrations were reduced 1.5- and 1.4-fold, respectively. The largest absolute depletion

was observed for Si with a reduction of 848 µmol $m^{-3}$ between early spring and summer. Conversely, summer SASW mixed-layer mean concentrations of $NO_3^-$, $PO_4^{3-}$ and Si were relatively 1.6, 1.4 and 2.1-fold lower than early spring, respectively, whilst the largest absolute depletion of 1912 µmol $m^{-3}$ was observed for $NO_3^-$. SASW mixed-layer concentrations of $NO_3^-$ and $PO_4^{3-}$ were at least 2.1-fold higher than for STSW during the study, whilst the Si concentration was at least 1.5-fold lower, highlighting the relative deficiencies in major nutrients between high and low latitude derived surface waters (Sarmiento et al., 2004; Moore, 2016).

***Sub-surface waters***

The Southern Ocean derived Sub-Antarctic Mode Water (SAMW) and underlying Antarctic Intermediate Water (AAIW) were identified using their characteristic core potential density ($\sigma\theta$ 26.8 kg $m^{-3}$) (Sarmiento et al., 2004; Palter et al., 2010) and thermohaline ($S$ <34.4, $\theta$ >2.8ºC) properties (Fig. 2). Wyatt et al. (2014) have identified these water masses along this section between 200 and 500 m. During all three transects, low sub-surface (50 – 500 m) macronutrient concentrations were observed between 13 and 16°E, associated with a salinity maxima. The feature conforms to the mean locality and depth range of Agulhas water (Duncombe Rae, 1991), clearly highlighting the penetration of Indian Ocean water into northward flowing SAMW.

### 3.2. Zn and Co distributions of the Southeast Atlantic Ocean

***Surface mixed-layer***

Figure 3 shows the dZn and dCo distributions for the upper 500 m of the Southeast Atlantic for the D357 and JCO68 transects. For full-depth dZn distributions along JC068 refer to Wyatt et al. (2014). In the surface mixed-layer, dZn and dCo concentrations ranged from 0.01 to 4.57

nM and 1 to 50 pM, respectively. The large range in dZn concentrations resulted from an apparent offshore transport of elevated dZn within STSW between 20 – 50 m during early spring (1.48 – 4.57 nM; Stns. 1 – 2) that was reduced by late spring (0.48 – 1.76 nM; Stns. 0.5 – 1.5) and was absent during summer (0.01 – 0.13 nM; Stns. 1 – 2). Similarly, but to a lesser extent, elevated dCo concentrations were observed in STSW between 10 and 50 m during early and late spring (15 – 50 pM), compared with summer (18 – 33 pM). Our findings are consistent with previous observations of elevated dissolved and particulate trace metals over the same depth range in waters close to South Africa, including Co, Fe, Mn, and Pb (Chever et al., 2010; Bown et al., 2011; Boye et al., 2012; Paul et al., 2015). We postulate that these trace metal enrichments can arise from either atmospheric inputs, and/or from the lateral advection of metal-enriched waters from the Agulhas Current (AC) and/or South African continental shelf, and discuss this further in Sect. 3.3. In SASW, mixed-layer dZn and dCo concentrations ranged from 0.01 to 0.25 nM and 3 to 18 pM, respectively, during the study, significantly lower than STSW values, with the lowest concentrations observed during the summer transect (Table 2).

***Sub-surface waters***

During the early spring D357-1 transect, elevated dZn and dCo concentrations were observed between the surface mixed-layer and 500 m (1.48–3.85 nM and 39–62 pM, respectively) at the station closest the South African continent (Stn. 1). Here, the highest dZn concentrations were associated with the dZn-enriched waters (20–55 m) described above for the surface mixed-layer. During the late spring D357-2 transect, the near-shore (Stns. 0.5–1) dZn concentrations were lower (0.31–1.76 nM) whilst dCo remained similar to early spring values (27–57 pM). During summer, near-shore (Stn. 1) sub-surface dZn concentrations were markedly lower (0.03–0.50 nM) than spring values whilst dCo concentrations (17–52 pM) were only marginally lower. In offshore waters, sub-surface dZn concentrations ranged from 0.01 to 1.01

311 nM across all three transects with extremely low values in the upper 400 m (0.22 ± 0.21 nM)
312 and the highest values between 400 and 500 m. The absence of a significant return path for
313 dZn with SAMW to waters above 400 m at this latitude (Wyatt et al., 2014; Vance et al., 2017)
314 is likely an important control on dZn distributions across all three transects. In contrast, dCo
315 concentrations were depleted in the upper 200 m (1–35 pM) and elevated in SAMW (23–56
316 pM) suggesting that these Southern Ocean derived waters also play an important role in upper
317 water column dCo distributions of the South Atlantic.
318 To assess whether seasonal changes in subsurface supply could influence dissolved Zn and Co
319 concentrations in the upper water column of the Southeast Atlantic, we examined the metal
320 versus $PO_4^{3-}$ distributions of underlying SAMW and AAIW. Throughout this paper metal:$PO_4^{3-}$
321 will be used to indicate an uptake remineralisation ratio derived from a regression slope, whilst
322 metal/$PO_4^{3-}$ will denote a concentration ratio. Figure 4 and supplementary table 1 show how
323 the dZn:$PO_4^{3-}$ regression slope for SAMW and AAIW varied little between the three transects.
324 These slopes are a function of the pre-formed micro- and macronutrient concentrations and the
325 uptake/remineralisation ratio of the sources waters, as well as mixing during advection between
326 the Southern Ocean and South Atlantic (Vance et al., 2017; Middag et al., 2018). The dZn:$PO_4^{3-}$
327 slopes steepen with the introduction of AAIW with higher dZn/$PO_4^{3-}$ concentration ratios, yet
328 it is the relatively shallow slopes of overlying SAMW that imply a low, and relatively
329 consistent, subsurface supply of dZn to STSW and SASW of the South Atlantic (Wyatt et al.,
330 2014). The shallower waters overlying SAMW clearly show elevated dZn concentration,
331 specifically during the spring transects, compared with what could be delivered if subsurface
332 supply was the dominant source governing dZn availability in surface waters (Fig. 4). It is
333 therefore unlikely that a change in subsurface supply from underlying SAMW is responsible
334 for the change in dZn inventories of STSW and SASW between the three transects.

Similarly, the dCo:$PO_4^{3-}$ regression slope varied little between the three transects (Fig. 4 and Supp. Table 1). In dCo:$PO_4^{3-}$ space, a single slope can be fit to SAMW and AAIW with no net scavenging effect on dCo distribution over the upper 1000 m. Like dZn, the waters overlying SAMW displayed spring dCo concentrations elevated above that potentially delivered via SAMW supply. During summer however, SAMW may provide a subsurface source of dCo (Fig. 4c) to overlying waters highlighting how Southern Ocean derived waters may play important, yet different, roles in upper water column metal distributions of the Southeast Atlantic.

### 3.3. Shelf derived sources of Zn and Co

Potential sources of trace metals to surface waters of the Southeast Atlantic include atmospheric inputs from South Africa and Patagonia (Chance et al., 2015; Menzel Barraqueta et al., 2019) as well as interactions with shelf and slope waters of the Agulhas Bank (Bown et al., 2011; Boye et al., 2012; Paul et al., 2015). During the D357 spring transects, elevated mixed-layer dZn and dCo concentrations (up to 4.57 nM and 50 pM, respectively; Sect. 3.2) were observed at stations closest the Agulhas Bank shelf and slope (Stns. 0.5, 1, 1.5 and 2). Here, we compare these metal elevations with respect to the aforementioned sources. Firstly, we encountered only brief, light rain during the study, thus minimal wet deposition of atmospheric aerosol. By combining the median atmospheric dry deposition flux for soluble Zn and Co for the Southeast Atlantic (Zn 6.0 and Co 0.05 nmol $m^{-2}$ $d^{-1}$; Chance et al., 2015) with the mean mixed-layer depth (34 m) for STSW during D357, dust dissolution is estimated to add approximately 5.5 and 0.05 nmol $m^{-3}$ dZn and dCo, respectively, over a one month period. These inputs are low compared with the mixed-layer metal inventories, representing <1 % of dZn and dCo concentration in STSW during the D357 transects (Table 2), and would not be sufficient to generate distinct mixed-layer maxima. It is likely, therefore, that the dZn and dCo

elevations originated from the advection of metal-enriched waters from the western Agulhas Bank, a region identified as a distinct source of both dissolved and particulate trace metals to the Southeast Atlantic (Chever et al., 2010; Bown et al., 2011; Boye et al., 2012; Paul et al., 2015), and/or from the leakage of Indian Ocean water into the Southeast Atlantic via the AC. The detachment of Agulhas rings and filaments from the AC during its retroflection back towards the Indian Ocean constitutes a source of Pb to the surface Southeast Atlantic along the D357 transects (Paul et al., 2015). Whilst we observed elevated mixed-layer dZn and dCo at ~15ºE during both D357 transects, the absence of metal enrichment across the depth of the AC salinity maxima (Figs. 2 and 3) suggests that the signal must be entrained from elsewhere. Furthermore, dZn concentrations from the AC along the east coast of South Africa do not exceed 0.5 nM in the upper 200 m (Gosnell et al., 2012). It is therefore likely that the dZn and dCo enrichment was derived from the Agulhas Bank. The AC has been shown to meander over, and interact with, the Agulhas Bank, forming eddies and filaments on the shoreward edge of the AC proper, that tend to move northwards along the western shelf edge and into the Southeast Atlantic (Lutjeharms and Cooper, 1996; Lutjeharms, 2007), potentially delivering shelf-derived sedimentary material. We found no evidence of a fluvial signature in our data, and no significant fluvial source for trace elements to our study region has been reported in the literature. We focus here on the more likely scenario of sedimentary inputs as the driver of mixed-layer dZn and dCo elevations at the shelf and slope stations during D357. Despite no available particulate trace metal data for the D357-1 early spring transect for direct comparison with the highest dZn and dCo elevations, we observed elevated mixed-layer particulate Zn (pZn; 0.08–1.40 nM) and Co (pCo; 8–49 pM) at stations closest South Africa during the D357-2 late spring transect (Stns. 0.5, 1 and 1.5, Fig. S1), coincident with elevated dZn (0.05–1.82 nM) and dCo (1–43 pM). Furthermore, for the upper 500 m at stations 0.5 and 1, we found strong positive correlations between particulate aluminium and titanium (pAl:pTi, slope 41.7

**Commented [NW3]:** This sentence has been condensed to avoid being repetitive.

385 mol $mol^{-1}$, Pearson's *r* 0.99, *n* = 15), as well as particulate Fe and titanium (pFe:pTi, slope 10.2
386 mol $mol^{-1}$, Pearson's *r* 0.99, *n* = 15), indicative of a strong lithogenic source. Whilst there are
387 presently no South African sedimentary data against which we can compare our water column
388 values, our pAl:pTi and pFe:pTi slope ratios are in excess of upper crustal mole ratios (34.1
389 and 7.3 mol $mol^{-1}$, respectively; Mclennan, 2001). These 500 m ratios are also steeper than the
390 aggregate slopes for the full depth Atlantic Ocean away from hydrothermal sources (32.1 and
391 7.4 mol $mol^{-1}$, Pearson's *r* >0.97, *n* = 593, Schlitzer, 2018). Given the refractory nature of
392 lithogenic pTi across diverse oceanic environments (Ohnemus and Lam, 2015), this may
393 suggest the resuspension and dissolution of Agulhas Bank sediments enriched in dAl and dFe,
394 followed by westward offshore transport, a common feature of the Bank's physical circulation
395 during spring and summer (Largier et al., 1992). Such processes may in turn provide an
396 additional source of dZn and dCo to STSW of the Southeast Atlantic. For example, Little et al.
397 (2016) proposed that oxygen-deficient, organic-rich, continental margin sediments may
398 constitute a significant global sink within the marine Zn cycle. These sediments could
399 additionally provide a local source of dZn following remineralisation. Recent model outputs
400 have likewise highlighted oxygen-deficient, boundary sediments as a dominant external source
401 of Co to the oceans (Tagliabue et al., 2018). Given that oxygen depleted (<45 µM) bottom
402 waters are prevalent across the western Agulhas Bank (Chapman and Shannon, 1987;
403 Chapman, 1988), considered to arise from high organic matter input to sediments and its
404 bacterial decomposition, a sedimentary source of dZn and dCo appears likely.
405
406 **3.4. Trace metal stoichiometry of the upper Southeast Atlantic**
407 In addition to seasonal variations in the lateral advection of continentally derived trace metals,
408 the lower dZn and dCo concentrations in STSW during summer, compared with spring, likely
409 reflect differences in biological utilisation. Here, we examine the micro- and macronutrient

concentration inventories to assess the trace metal stoichiometry of the Southeast Atlantic over seasonal timescales. The data were grouped into STSW and SASW regimes, with STSW defined by $\theta \geq 15$°C. This isotherm was located at a mean depth of 144 ± 96 m across the study, compared with a mean mixed-layer depth of 39 ± 10 m, and thus the inventories for SASW were determined over this depth for comparison with STSW (Table 2). Early and late spring STSW samples in the depth range 20 - 55 m that clearly exhibited continentally derived elevated dZn and dCo were removed from the analysis in order to compare stoichiometry with respect to biological processes. For SASW, micronutrient sampling did not occur during late spring and therefore only early spring and summer values are compared.

Distinct temporal trends in the stoichiometric relationship with $PO_4^{3-}$ were evident for both dZn and dCo (Fig. 4). Within STSW, the dZn/$PO_4^{3-}$ inventory ratio ranged from 699 to 1876 µmol $mol^{-1}$ (Table 2) with the highest value observed during early spring and the lowest during summer. Combined with summer dZn concentrations 4-fold lower than early spring, this suggests strong biological uptake of dZn alongside $PO_4^{3-}$ between seasons. In contrast, lower dZn/$PO_4^{3-}$ ratios of 372 and 188 µmol $mol^{-1}$ were observed in SASW during early spring and summer, respectively. Here, the absolute change in dZn concentration between spring and summer was lower than for STSW, but was greater for $PO_4^{3-}$, likely reflecting the increased availability of $PO_4^{3-}$ in these Southern Ocean derived waters (Table 2) and an open-ocean phytoplankton community that have lower trace metal requirements than their counterparts north of the STF. Such dZn/$PO_4^{3-}$ ratios sit at the lower end of cellular Zn/P reported for the diatom and haptophyte-type phytoplankton typical of this region (~100 – 1100 µmol $mol^{-1}$; Twining and Baines, 2013 and refs. therein), highlighting the importance of micronutrient processes with respect to Zn availability.

In contrast to dZn, the spatiotemporal variation observed for STSW dCo/$PO_4^{3}$ was small with ratios ranging from 82 to 129 µmol $mol^{-1}$ (Table 2), likely reflecting external inputs to the

**Commented [NW4]:** Here we have made clear that STSW was defined on a station-by-station basis using 15 C whereas SASW was defined by the mean depth of 15 C for the entire study.

oceans and biological Co requirements that are typically 4-fold less than for Zn (Ho et al., 2003; Roshan et al., 2016; Hawco et al., 2018). The STSW $dCo/PO_4^{3-}$ ratio decreased between early and late spring transects, potentially in part due to the westward expansion of STSW during late spring (Fig. 2) and subsequent mixing with SASW depleted in dCo relative to $PO_4^{3-}$ (Fig. 3). This dilution is likely also true of dZn and Si, yet their STSW concentration inventories may be sufficiently high as to mask this effect. Unfortunately, an insufficient quantity of late spring SASW data are available with which to affirm this postulation. The highest $dCo/PO_4^{3-}$ ratio was observed during summer due to the preferential biological removal of $PO_4^{3-}$ relative to dCo.

In SASW, $dCo/PO_4^{3-}$ was consistently low with ratios of 23 and 26 µmol $mol^{-1}$ for early spring and summer, respectively. Much higher inventory ratios of ~580 µmol $mol^{-1}$ can be calculated over similar depths for open-ocean North Atlantic waters (GA03 Stns. 11-20, Schlitzer et al., 2018), likely reflecting an elevated atmospheric Co input and/or an extremely low surface $PO_4^{3-}$ inventory (Wu et al., 2000; Martiny et al., 2019).

Our results provide evidence for the greater availability and preferential removal of dZn relative to dCo in the upper water column the Southeast Atlantic based on STSW dZn/dCo inventory ratios of 19, 17 and 5 mol $mol^{-1}$ for the three transects and SASW ratios of 13 and 7 mol $mol^{-1}$ for early spring and summer, respectively (Table 2). With relatively consistent inter-seasonal dCo inventories for STSW and SASW, indicating a more balanced ecophysiological regime with regard to dCo organisation, the change in dZn/dCo inventory stoichiometries principally reflects changes in dZn concentration. We postulate that the inter-seasonal variations in dZn and dCo availability and stoichiometry of the Southeast Atlantic reflect changes in the relative nutritional requirement of resident phytoplankton and/or biochemical substitution of Zn and Co to meet nutritional demand.

### 3.5. Phytoplankton controls on trace metal ecological stoichiometry

Here we discuss the principle phenomena that together likely explain our observations of seasonally decreasing dZn/dCo inventory stoichiometries in STSW and SASW of the Southeast Atlantic: i.e. the preferential removal of dZn, relative to dCo, leading to low dZn availability, and differences in phytoplankton assemblages with different cellular metal requirements.

Satellite images show elevated surface chlorophyll concentrations across the Southeast Atlantic STF, compared with waters further north and south, with peak concentrations observed during summer in January 2012 (Fig. 1). Profiles of total chlorophyll-*a* concentration (Fig. S2) also show maximum summer values in the upper water column of STSW (1.02 mg $m^{-3}$) and SASW (0.49 mg $m^{-3}$) compared with spring values (<0.61 and <0.36 mg $m^{-3}$, respectively). This is consistent with the hypothesis that increasing irradiance, coupled with shallower mixed-layer depths (de Boyer Montégut et al., 2004), result in enhanced growth conditions across the STF between September and February (Browning et al., 2014). Diagnostic pigment analyses (Fig. 5a) indicated that eukaryotic nanophytoplankton, specifically *Phaeocystis*-type haptophytes, dominated the early spring STSW chlorophyll-*a* content (73 %) but with a reduced contribution during summer (20 %). Maximum growth rates for cultured *Phaeocystis antarctica* have been achieved under elevated Zn concentrations (Saito and Goepfert, 2008), and thus, the dominance of this haptophyte would likely contribute to the removal of dZn between spring and summer. Furthermore, an increased summer diatom contribution (13 % chlorophyll-*a* compared with near zero during spring transects) would have further reduced the dZn inventory, with diatoms having at least 4-fold higher cellular Zn/P ratios than co-occurring cell types (Twining and Baines, 2013).

The fact that both *Phaeocystis* and diatomaceous nanophytoplankton maintain a contribution to the summer STSW chlorophyll-*a* complement, when dZn availability is low, is intriguing.

485 Both *P. antarctica* and the large, coastal diatoms *Thalassiosira pseudonana* and *Thalassiosira*
486 *weissflogii* have been shown to be growth limited in culture by free $Zn^{2+}$ concentrations ≤10
487 pM (Sunda and Huntsman, 1992; Saito and Goepfert, 2008). A simple estimate of summer
488 STSW free $Zn^{2+}$ availability, based on North Atlantic organic complexation data (>96 %;
489 Ellwood and Van den Berg, 2000), indicated free $Zn^{2+}$ averaged $6.3 \pm 5.3u_c$ pM, suggesting the
490 potential for growth limitation of these phytoplankton. In addition, when comparing the
491 Southeast Atlantic dZn stoichiometry with the cellular requirements of phytoplankton grown
492 under growth rate limiting conditions (Fig. 6), we found summer STSW $dZn/PO_4^{3-}$ to be in
493 deficit of the requirements of coastal *T. pseudonana* but not those of the smaller, open-ocean
494 diatom *T. oceanica*. The variation in cellular Zn/P between small and large phytoplankton is
495 related to the higher surface-area-to-volume ratio of smaller cells, and the limitation of
496 diffusive uptake rates at low $Zn^{2+}$ concentrations (Sunda and Huntsman, 1995). This would
497 suggest that the lower dZn availability in summer STSW should influence phytoplankton
498 species composition by selecting for smaller organisms with lower cellular Zn requirements,
499 and confirmed by a ratio of picophytoplankton to nanophytoplankton at least 4-fold higher
500 during summer compared with spring values. The comparison further implies that the presence
501 of *Phaeocystis* and diatoms in summer STSW may be linked with their metabolic Zn-Co-Cd
502 substitution capability, potentially allowing them to overcome some portion of their Zn
503 deficiency. Largely connected to carbonic anhydrase enzymes, several species of eukaryotic
504 phytoplankton are capable of biochemical substitution of Zn, Co or Cd to maintain optimal
505 growth rates under low trace metal conditions (Price and Morel, 1990; Sunda and Huntsman,
506 1995; Lee and Morel, 1995; Lane and Morel, 2000; Xu et al., 2007; Saito and Goepfert, 2008;
507 Kellogg et al., 2020). For example, metabolic substitution of Co in place of Zn has been
508 observed to support the growth of *P. antarctica*, *T. pseudonana* and *T. weissflogii* in media
509 with $Zn^{2+}$ <3 pM (Sunda and Huntsman, 1995; Saito and Goepfert, 2008; Kellogg et al., 2020).

Thus, the lower mixed-layer dCo inventory of summer STSW, relative to early spring, may be in part related to enhanced dCo uptake through biochemical substitution alongside the growth of phytoplankton with distinct Co requirements.

In contrast to *Phaeocystis*, *E. huxleyi*-type haptophytes were near-absent in spring STSW (<5 % chlorophyll-*a*; Fig. 5a) and increased in contribution during summer (18 %). *Emiliania huxleyi* appear to have a biochemical preference for Co over Zn (Xu et al., 2007), which could potentially be a contributing factor to the increased fraction of this haptophyte in summer STSW. Based on Co organic complexation data for Southeast Atlantic STSW (>99 %; Bown et al., 2012), however, even the maximum dCo concentration of 56 pM (estimated free $Co^{2+}$ 0.56 ± 0.11$u_c$ pM) observed for STSW during this entire study would limit the growth of cultured *E. huxleyi* in the absence of Zn or Cd (Sunda and Huntsman, 1995; Xu et al., 2007). This is supported by inter-seasonal dCo/$PO_4^{3-}$ stoichiometries in deficit of the cellular requirements of cultured *E. huxleyi* (Fig. 6). Despite this, Xu et al. (2007) showed that *E. huxleyi* can maintain significant growth at only 0.3 pM $Co^{2+}$ in the presence of Zn, with the limitation by, and substitution of these metals reported to occur over a range of free ion concentrations (0.2–5 pM) that is relevant to summer conditions of the Southeast Atlantic. This assessment implies an additional need for Zn in phytoplankton nutrition due to low dCo availability throughout the Southeast Atlantic, which may accelerate the decrease in dZn/dCo inventory ratio between seasons.

The elevated summer STSW chlorophyll-*a* concentrations were accompanied by increased cell concentrations of the *Synechococcus* and *Prochlorococcus* (up to 100 and 400 cells $\mu L^{-1}$, respectively) relative to early spring abundance (Fig. 5b). This pattern suggests an inter-seasonal community shift towards smaller picocyanobacterial cells that is coincident with decreased dZn availability. *Synechococcus* and *Prochlorococcus* are thought to have little or no Zn requirement and relatively low Co requirements (growth limited by ≤0.2 pM $Co^{2+}$; Sunda

and Huntsman, 1995; Saito et al., 2002). This, alongside their small cell size, hence greater capacity for acquiring fixed nitrogen under conditions where this nutrient is depleted, may allow these prokaryotes to flourish following depletion and export of Zn associated with *Phaeocystis* and diatom blooms. This supposition is supported by a persistently high abundance of *Synechococcus* and *Prochlorococcus* (>1000 cells $\mu L^{-1}$), relative to eukaryotic nanophytoplankton, in the dZn depleted surface waters of the Costa Rica Dome (Saito et al., 2005; Ahlgren et al., 2014; Chappell et al., 2016). Here, surface dCo concentrations were maintained above that of surrounding waters by the biological production of Co-binding ligands (Saito et al., 2005). The increased abundance of these prokaryotic autotrophs in summer STSW of the Southeast Atlantic may have also contributed to the inter-seasonal decrease in dCo inventory.

In contrast to STSW, cells counts of eukaryotic phytoplankton and prokaryotic cyanobacteria in SASW varied little between early spring and summer (Fig. 5b), indicative of a more balanced ecophysiological regime. The fractional contribution of *Phaeocystis* (Fig. 5a), the dominant contributor to the SASW chlorophyll-*a* complement, was similar between transects at 54 and 44 %, respectively, whilst the contribution of *E. huxleyi* increased from 19 to 33 % between spring and summer, respectively. Whilst it is proposed that the low Fe supply rate to these waters provides a dominant control on phytoplankton biomass and composition (Browning et al., 2014), low dZn and dCo availability may also be important drivers of such change. The Summer SASW dZn inventory ($0.08 \pm 0.07u_c$ nM) and stoichiometry with $PO_4^{3-}$ (Fig. 6) indicate growth limiting conditions for *Phaeocystis* and *E. huxleyi* in the absence of cambialistic metabolism (Sunda and Huntsman., 1995; Saito and Goepfert, 2008; Xu et al., 2007). The presence of these phytoplankton therefore indicates Zn biochemical substitution occur in oceanic waters of the Southeast Atlantic. A lower Co half-saturation growth constant for cultured *P. antarctica* ($K_m$ = ~0.2 pM $Co^{2+}$), compared with *E. huxleyi* ($K_m$ = ~3.6 pM

560 $Co^{2+}$), further suggests that *Phaeocystis* species may more effectively occupy low dZn and dCo
561 environments (Saito and Goepfert, 2008), such as SASW of the South Atlantic.
562 Conversely, the absence of a significant diatom contribution to summer SASW chlorophyll-*a*
563 (Fig. 5a), relative to early spring, is surprising as the summer $dZn/PO_4^{3-}$ inventory ratio is in
564 excess of the cellular Zn/P requirements of typical oceanic diatoms such as *T. oceanica* (Fig.
565 6). Furthermore, whilst the $dCo/PO_4^{3-}$ ratio of summer SASW is in deficit of the cellular Co/P
566 below which growth limitation of *T. oceanica* may occur, this species has been shown to grow
567 effectively at $Co^{2+}$ <0.1 pM in culture in the presence of Zn (Sunda and Huntsman, 1995). The
568 low diatom fractional contribution to summer SASW may be instead related to low Fe
569 availability (Browning et al., 2014) and stress-induced Si exhaustion. In support of this, we
570 calculate summer SASW mixed-layer Si concentrations (0.9 ± 0.3 µM) to be 50 % of early
571 spring values (1.8 ± 0.2 µM) with a dissolved $NO_3^-$/Si stoichiometry of 3.8 mol $mol^{-1}$ close to
572 the 4 mol $mol^{-1}$ shown to limit diatom growth in culture (Gilpin et al., 2004), and in contrast to
573 the 2.9 mol $mol^{-1}$ calculated for early spring.
574

575 **3.6. Conclusion**

576 We report the distributions of dZn and dCo in the upper water column of sub-tropical and sub-
577 Antarctic waters of the Southeast Atlantic during austral spring and summer periods. We
578 identify an apparent continental source of dZn and dCo to sub-tropical waters at depths between
579 20 – 55 m, derived from sedimentary inputs from the Agulhas Bank. In contrast, open-ocean
580 sub-Antarctic surface waters displayed largely consistent inter-seasonal mixed-layer dZn and
581 dCo concentrations indicating a more balanced ecophysiological regime with regard to their
582 organisation. The vertical distributions of dZn and dCo in the upper water column were similar
583 to that of $PO_4^{3-}$ indicating biological drawdown in surface waters and mixing with underlying
584 Southern ocean-derived waters travelling equatorward significantly influences their

**Commented [NW5]:** We have corrected this sentence on the advice of reviewer 1. Previously it felt incomplete.

**Commented [NW6]:** We have clarified that T oceanica are able to grow at low Co in the presence of Zn.

distribution. Absolute trace metal concentrations alongside concentration inventory ratios suggest the preferential utilization of dZn, relative to dCo, in the Southeast Atlantic with dZn/dCo decreasing from 19 to 5 mol $mol^{-1}$ between early spring and summer in STSW and from 13 to 7 mol $mol^{-1}$ in SASW. This pattern is consistent with our understanding of the cellular requirement of phytoplankton (Twining and Baines, 2013). The inter-seasonal removal of dZn results in summer concentrations that are potentially growth limiting for certain phytoplankton species estimated to be present in these waters by diagnostic pigment analyses. We therefore suggest cambialistic metabolic substitution between Zn and Co, and potentially Cd, is an important factor regulating the growth, distribution and diversity of phytoplankton in the Southeast Atlantic.

*Data availability.* The trace metal and macronutrient data sets used for analyses in this study are available at https://www.bodc.ac.uk/geotraces/data/idp2017/ (GEOTRACES GA10) and phytoplankton data at https://www.bodc.ac.uk/.

*Competing interests*. The authors declare that they have no conflict of interest.

*Author contribution.* MCL and EPA acquired the funding. NJW, MCL, AM, TJB, EMSW, and HAB collected samples at sea. NJW conducted the Zn and Co measurements, EMSW the macronutrient measurements and TJB the phytoplankton measurements. NJW prepared the manuscript with significant contributions from all co-authors.

*Acknowledgments.* We thank the officers, crew, technicians and scientists of the *RRS James Cook* for their help on the UK-GEOTRACES D357 and JC068 cruises. This work was funded

609 by the UK-GEOTRACES National Environmental Research Council (NERC) Consortium
610 Grant (NE/H006095/1 (MCL & HAB) & NE/H004475/1 (EPA)).

611

612 References

613 Ahlgren, N. A., Noble, A. E., Patton, A. P., Roache-Johnson, K., Jackson, L., Robinson, D.,
614 McKay, C., Moore, L. R., Saito, M. A., and Rocap, G.: The unique trace metal and mixed layer
615 conditions of the Costa Rica upwelling dome support a distinct and dense community of
616 Synechococcus, Limnol. Oceanogr., 59, 2166-2184, doi:10.4319/lo.2014.59.6.2166, 2014.

617 Ansorge, I. J., Speich, S., Lutjeharms, J. R. E., Goni, G. J., Rautenbach, C. J. D., Froneman, P.
618 W., Rouault, M., and Garzoli, S.: Monitoring the oceanic flow between Africa and Antarctica:
619 Report of the first Goodhope cruise, S. Afr. J. Sci., 101, 29-35, 2005.

620 Bertrand, E. M., Saito, M. A., Rose, J. M., Riesselman, C. R., Lohan, M. C., Noble, A. E., Lee,
621 P. A., and DiTullio, G. R.: Vitamin b12 and iron colimitation of phytoplankton growth in the
622 Ross Sea, Limnol. Oceanogr., 52, 1079-1093, doi:10.4319/lo.2007.52.3.1079, 2007.

623 Bown, J., Boye, M., Baker, A., Duvieilbourg, E., Lacan, F., Le Moigne, F., Planchon, F.,
624 Speich, S., and Nelson, D. M.: The biogeochemical cycle of dissolved cobalt in the Atlantic
625 and the Southern Ocean south off the coast of South Africa, Mar. Chem., 126, 193-206,
626 doi:10.1016/j.marchem.2011.03.008, 2011.

627 Bown, J., Boye, M., and Nelson, D. M.: New insights on the role of organic speciation in the
628 biogeochemical cycle of dissolved cobalt in the southeastern Atlantic and the Southern Ocean,
629 Biogeosciences, 9, 2719–2736, doi:10.5194/bg-9-2719-2012, 2012.

630 Boye, M., Wake, B. D., Garcia, P. L., Bown, J., Baker, A. R., and Achterberg, E. P.:
631 Distributions of dissolved trace metals (Cd, Cu, Mn, Pb, Ag) in the southeastern Atlantic and
632 the Southern Ocean, Biogeosciences, 9, 3231-3246, doi:10.5194/bg-9-3231-2012, 2012.

633 Browning, T. J., Bouman, H. A., Moore, C. M., Schlosser, C., Tarran, G. A., Woodward, E.
634 M. S., and Henderson, G. M.: Nutrient regimes control phytoplankton ecophysiology in the
635 South Atlantic, Biogeosciences, 11, 463-479, doi:10.5194/bg-11-463-2014, 2014.

636 Browning, T. J., Achterberg, E. P., Rapp, I., Engel, A., Bertrand, E. M., Tagliabue, A., and
637 Moore, C. M.: Nutrient co-limitation at the boundary of an oceanic gyre, Nature, 551, 242-246,
638 doi:10.1038/nature24063, 2017.

639 Cannizzaro, V., Bowie, A.R., Sax, A., Achterberg, E. P., Worsfold, P. J.: Determination of
640 cobalt and iron in estuarine and coastal waters using flow injection with chemiluminescence
641 detection, Analyst, 125, 51-57, doi:10.1039/A907651d, 2000.

642 Carritt, D. E., and Carpenter, J. H.: Comparison and evaluation of currently employed
643 modifications of the Winkler method for determining dissolved oxygen in seawater; a nasco
644 report, J. Mar. Res., 24, 286 - 319, 1966.

Chance, R., Jickells, T. D., and Baker, A. R.: Atmospheric trace metal concentrations, solubility and deposition fluxes in remote marine air over the south-east Atlantic, Mar. Chem., 177, 45-56, doi:10.1016/j.marchem.2015.06.028, 2015.

Chapman, P.: On the occurrence of oxygen-depleted water south of Africa and its implications for Agulhas-Atlantic mixing, S. Afr. J. Marine Sci., 7, 267-294, doi:10.2989/025776188784379044, 1988.

Chapman, P., and Shannon, L. V.: Seasonality in the oxygen minimum layers at the extremities of the Benguela system, S. Afr. J. Marine Sci., 5, 85-94, doi:10.2989/025776187784522162, 1987.

Chappell, P. D., Vedmati, J., Selph, K. E., Cyr, H. A., Jenkins, B. D., Landry, M. R., and Moffett, J. W.: Preferential depletion of zinc within Costa Rica upwelling dome creates conditions for zinc co-limitation of primary production, J. Plankton Res., 38, 244-255, doi:10.1093/plankt/fbw018, 2016.

Chever, F., Bucciarelli, E., Sarthou, G., Speich, S., Arhan, M., Penven, P., and Tagliabue, A.: Physical speciation of iron in the Atlantic sector of the Southern Ocean along a transect from the subtropical domain to the Weddell Sea Gyre, J. Geophys. Res-Oceans, 115, C10059, doi:10.1029/2009jc005880, 2010.

Cox, A., and Saito, M.: Proteomic responses of oceanic Synechococcus WH8102 to phosphate and zinc scarcity and cadmium additions, Front Microbiol, 4, doi:10.3389/fmicb.2013.00387, 2013.

Cullen, J. T., and Sherrell, R. M.: Effects of dissolved carbon dioxide, zinc, and manganese on the cadmium to phosphorus ratio in natural phytoplankton assemblages, Limnol. Oceanogr., 50, 1193-1204, doi:10.4319/lo.2005.50.4.1193, 2005.

Davey, M., Tarran, G. A., Mills, M. M., Ridame, C., Geider, R. J., and LaRoche, J.: Nutrient limitation of picophytoplankton photosynthesis and growth in the tropical North Atlantic, Limnol. Oceanogr., 53, 1722–1733, doi:10.4319/lo.2008.53.5.1722, 2008

de Boyer Montégut, C., Madec, G., Fischer, A. S., Lazar, A., and Iudicone, D.: Mixed layer depth over the global ocean: An examination of profile data and a profile-based climatology, J. Geophys. Res-Oceans, 109, C12003, doi:10.1029/2004jc002378, 2004.

Dulaquais, G., Boye, M., Middag, R., Owens, S., Puigcorbe, V., Buesseler, K., Masqué, P., Baar, H. J., and Carton, X.: Contrasting biogeochemical cycles of cobalt in the surface western Atlantic Ocean, Global Biogeochem. Cy., 28, 1387–1412, doi:10.1002/2014GB004903, 2014.

Duncombe Rae, C. M.: Agulhas retroflection rings in the South Atlantic Ocean: An overview, S. Afr. J. Marine Sci., 11, 327-344, doi:10.2989/025776191784287574, 1991.

Ellwood, M. J., and Van den Berg, C. M. G.: Zinc speciation in the Northeastern Atlantic Ocean, Mar. Chem., 68, 295-306, doi:10.1016/S0304-4203(99)00085-7, 2000.

Franck, V. M., Bruland, K. W., Hutchins, D. A., and Brzezinski, M. A.: Iron and zinc effects on silicic acid and nitrate uptake kinetics in three high-nutrient, low-chlorophyll (HNLC) regions, Mar. Ecol. Prog. Ser., 252, 15-33, doi:10.3354/meps252015, 2003.

Gilpin, L. C., Davidson, K., and Roberts, E.: The influence of changes in nitrogen: silicon ratios on diatom growth dynamics, J. Sea Res., 51, 21-35, doi:10.1016/j.seares.2003.05.005, 2004.

Gosnell, K. J., Landing, W. M., and Milne, A.: Fluorometric detection of total dissolved zinc in the southern Indian Ocean, Mar. Chem., 132, 68-76, doi:10.1016/j.marchem.2012.01.004, 2012.

Hawco, N. J., and Saito, M. A.: Competitive inhibition of cobalt uptake by zinc and manganese in a Pacific Prochlorococcus strain: Insights into metal homeostasis in a streamlined oligotrophic cyanobacterium, Limnol. Oceanogr., 63, 2229-2249, doi:10.1002/lno.10935, 2018.

Hawco, N.J., Lam, P.J., Lee, J.M., Ohnemus, D.C., Noble, A.E., Wyatt, N.J., Lohan, M.C., and Saito M.A.: Cobalt scavenging in the mesopelagic ocean and its influence on global mass balance: synthesizing water column and sedimentary fluxes, Mar. Chem., 201, 151-166, doi.org/10.1016/j.marchem.2017.09.001, 2018.

Ho, T. Y., Quigg, A., Finkel, Z. V., Milligan, A. J., and Wyman, K.: The elemental composition of some marine phytoplankton, J. Phycol., 39, 1145-59, doi.org/10.1111/j.0022-3646.2003.03-090.x.

Holm-Hansen, O., Lorenzen, C. J., and Holmes, J. D. H.: Fluorometric determination of chlorophyll, ICES J. Mar. Sci., 30, 3-15, doi.org/10.1093/icesjms/30.1.3, 1965.

Ito, T., Parekh, P., Dutkiewicz, S., and Follows, M. J.: The Antarctic circumpolar productivity belt, Geophys. Res. Lett., 32, L13604, doi:10.1029/2005gl023021, 2005.

Jakuba, R. W., Moffett, J. W., and Dyhrman, S. T.: Evidence for the linked biogeochemical cycling of zinc, cobalt, and phosphorus in the western north Atlantic Ocean, Global Biogeochem. Cy., 22, GB4012, doi:10.1029/2007GB003119, 2008.

Jakuba, R. W., Saito, M. A., Moffett, J. W., and Xu, Y.: Dissolved zinc in the subarctic North Pacific and Bering Sea: Its distribution, speciation, and importance to primary producers, Global Biogeochem. Cy., 26, GB2015, doi:10.1029/2010gb004004, 2012.

Kellogg, M.M., Mcllvin, M.R., Vedamati, J.,Twining, B.S., Moffett, J.W., Marchetti, A., Moran, D.M., and Saito, M.A.: Efficient zinc/cobalt inter-replacement in northeast Pacific diatoms and relationship to high surface dissolved Co:Zn ratios, Limnol. Oceanogr., 9999, 1-26, doi:10.1002/lno.11471, 2020.

Lane, T. W., and Morel, F. M. M.: Regulation of carbonic anhydrase expression by zinc, cobalt, and carbon dioxide in the marine diatom Thalassiosira weissflogii, Plant Physiol., 123, 345-352, doi:10.1104/Pp.123.1.345, 2000.

Largier, J. L., Chapman, P., Peterson, W. T., and Swart, V. P.: The western Agulhas Bank: circulation, stratification and ecology, S Afr J Marine Sci, 12, 319-339, doi:10.2989/02577619209504709, 1992.

Leblanc, K., Hare, C. E., Boyd, P. W., Bruland, K. W., Sohst, B., Pickmere, S., Lohan, M. C., Buck, K., Ellwood, M., and Hutchins, D. A.: Fe and Zn effects on the Si cycle and diatom community structure in two contrasting high and low-silicate HNLC areas, Deep-Sea Res. Pt I, 52, 1842-1864, doi:10.1016/j.dsr.2005.06.005, 2005.

Lee, J. G., and Morel, F. M. M.: Replacement of zinc by cadmium in marine phytoplankton, Mar. Ecol. Prog. Ser., 127, 305-309, doi:10.3354/Meps127305, 1995.

Little, S. H., Vance, D., McManus, J., and Severmann, S.: Key role of continental margin sediments in the oceanic mass balance of Zn and Zn isotopes, Geology, 44, 207-210, doi:10.1130/G37493.1, 2016.

Lutjeharms, J. R. E.: Three decades of research on the greater Agulhas Current, Ocean Sci., 3, 129-147, doi:10.5194/os-3-129-2007, 2007.

Lutjeharms, J. R. E., and Cooper, J.: Interbasin leakage through Agulhas current filaments, Deep-Sea Res. Pt I, 43, 213-238, doi:10.1016/0967-0637(96)00002-7, 1996.

Mackey, M. D., Mackey, D. J., Higgins, H. W., and Wright, S. W.: Chemtax - a program for estimating class abundances from chemical markers: Application to HPLC measurements of phytoplankton, Mar. Ecol. Prog. Ser., 144, 265-283, doi:10.3354/meps144265, 1996.

Mahaffey, C., Reynolds, S., Davis, C. E., and Lohan, M. C.: Alkaline phosphatase activity in the subtropical ocean: Insights from nutrient, dust and trace metal addition experiments, Front. Mar. Sci., 1, doi:10.3389/fmars.2014.00073, 2014.

Martiny, A. C., Lomas, M. W., Fu, W., Boyd, P. W., Chen, Y. L., Cutter, G. A., Ellwood, M. J., Furuya, K., Hashihama, F., Kanda, J., Karl, D. M., Kodama, T., Li, Q. P., Ma, J., Moutin, T., Woodward, E. M. S., and Moore, J. K.: Biogeochemical controls of surface ocean phosphate, Sci. Adv., 5, eaax0341, doi:10.1126/sciadv.aax0341, 2019.

McLennan, S. M.: Relationships between the trace element composition of sedimentary rocks and upper continental crust, Geochem. Geophy. Geosy., 2, doi:10.1029/2000gc000109, 2001.

Menzel Barraqueta, J. L., Klar, J. K., Gledhill, M., Schlosser, C., Shelley, R., Planquette, H. F., Wenzel, B., Sarthou, G., and Achterberg, E. P.: Atmospheric deposition fluxes over the Atlantic Ocean: A GEOTRACES case study, Biogeosciences, 16, 1525-1542, doi:10.5194/bg-16-1525-2019, 2019.

Middag, R., de Barr, H.J.W., and Bruland, K.W.: The relationships between dissolved zinc and major nutrients phosphate and silicate along the GEOTRACES GA02 transect in the western Atlantic Ocean, Global Biogeochem. Cy., 33, 63-84, doi.org/10.1029/2018GB006034, 2019.

Milne, A. C., Schlosser, C., Wake, B. D., Achterberg, E. P., Chance, R., Baker, A. R., Forryan, A., and Lohan, M. C.: Particulate phases are key in controlling dissolved iron concentrations in the (sub)tropical North Atlantic, Geophys. Res. Lett., 44, 2377-2387, doi:10.1002/2016GL072314, 2017.

Moore, C. M.: Diagnosing oceanic nutrient deficiency, Philisophical Transactions of the Royal Society A: Mathmatical, Physical and Engineering Sciences, 374, doi:10.1098/rsta.2015.0290, 2016.

Moore, C. M., Mills, M. M., Arrigo, K. R., Berman-Frank, I., Bopp, L., Boyd, P. W., Galbraith, E. D., Geider, R. J., Guieu, C., Jaccard, S. L., Jickells, T. D., La Roche, J., Lenton, T. M., Mahowald, N. M., Marañón, E., Marinov, I., Moore, J. K., Nakatsuka, T., Oschlies, A., Saito, M. A., Thingstad, T. F., Tsuda, A., and Ulloa, O.: Processes and patterns of oceanic nutrient limitation, Nat. Geosci., 6, 701-710, doi:10.1038/ngeo1765, 2013.

764 Moore, J. K., and Abbott, M. R.: Phytoplankton chlorophyll distributions and primary
765 production in the Southern Ocean, J. Geophys. Res-Oceans, 105, 28709-28722,
766 doi:10.1029/1999jc000043, 2000.

767 Morel, F. M. M.: The co-evolution of phytoplankton and trace element cycles in the oceans,
768 Geobiology, 6, 318-324, doi:10.1111/j.1472-4669.2008.00144.x, 2008.

769 Morel, F. M. M., Reinfelder, J. R., Roberts, S. B., Chamberlain, C. P., Lee, J. G., and Yee, D.:
770 Zinc and carbon co-limitation of marine-phytoplankton, Nature, 369, 740-742,
771 doi:10.1038/369740a0, 1994.

772 Noble, A. E., Ohnemus, D. C., Hawco, N. J., Lam, P. J., and Saito, M. A.: Coastal sources,
773 sinks and strong organic complexation of dissolved cobalt within the US North Atlantic
774 GEOTRACES transect GA03, Biogeosciences, 14, 2715–2739, doi:10.5194/bg-14-2715-
775 2017, 2017.

776 Ohnemus, D. C., and Lam, P. J.: Cycling of lithogenic marine particles in the US
777 GEOTRACES North Atlantic transect, Deep-Sea Res. Pt II, 116, 283-302,
778 doi:10.1016/j.dsr2.2014.11.019, 2015.

779 Ohnemus, D. C., Auro, M. E., Sherrell, R. M., Lagerstrom, M., Morton, P. L., Twining, B. S.,
780 Rauschenberg, S., and Lam, P. J.: Laboratory intercomparison of marine particle digestions
781 including Piranha: A novel chemical method for dissolution of polyethersulfone filters,
782 Limnol. Oceanogr-Meth., 12, 530-547, doi:10.4319/lom.2014.12.530, 2014.

783 Palter, J. B., Sarmiento, J. L., Gnanadesikan, A., Simeon, J., and Slater, R. D.: Fueling export
784 production: nutrient return pathways from the deep ocean and their dependence on the
785 Meridional Overturning Circulation, Biogeosciences, 7, 3549-3568, doi:10.5194/bg-7-3549-
786 2010, 2010.

787 Paul, M., van de Flierdt, T., Rehkämper, M., Khondoker, R., Weiss, D., Lohan, M. C., and
788 Homoky, W. B.: Tracing the Agulhas leakage with lead isotopes, Geophys. Res. Lett., 42,
789 8515-8521, doi:10.1002/2015gl065625, 2015.

790 Price, N. M., and Morel, F. M. M.: Cadmium and cobalt substitution for zinc in a marine
791 diatom, Nature, 344, 658-660, doi:10.1038/344658a0, 1990.

792 Raux, E., Schubert, H. L., and Warren*, M. J.: Biosynthesis of cobalamin (vitamin B12): A
793 bacterial conundrum, Cell. Mol. Life Sci., 57, 1880-1893, doi:10.1007/PL00000670, 2000.

794 Rodionov, D. A., Vitreschak, A. G., Mironov, A. A., and Gelfand, M. S.: Comparative
795 genomics of the vitamin B12 metabolism and regulation in prokaryotes, J. Biol. Chem., 278,
796 41148-41159, doi:10.1074/jbc.M305837200, 2003.

797 Saito, M. A., and Goepfert, T. J.: Zinc-cobalt colimitation of Phaeocystis antarctica, Limnol.
798 Oceanogr., 53, 266-275, doi:10.4319/lo.2008.53.1.0266, 2008.

799 Saito, M. A., and Moffett, J. W.: Temporal and spatial variability of cobalt in the Atlantic
800 Ocean, Geochim. Cosmochim. Ac., 66, 1943-1953, doi:10.1016/S0016-7037(02)00829-3,
801 2002.

802 Saito, M. A., Rocap, G., and Moffett, J. W.: Production of cobalt binding ligands in a
803 Synechococcus feature at the Costa Rica upwelling dome, Limnol. Oceanogr., 50, 279-290,
804 doi:10.4319/lo.2005.50.1.0279, 2005.

805 Saito, M. A., Moffett, J. W., Chisholm, S. W., and Waterbury, J. B.: Cobalt limitation and
806 uptake in Prochlorococcus, Limnol. Oceanogr., 47, 1629-1636,
807 doi:10.4319/lo.2002.47.6.1629, 2002.

808 Saito, M. A., Goepfert, T. J., Noble, A. E., Bertrand, E. M., Sedwick, P. N., and DiTullio, G.
809 R.: A seasonal study of dissolved cobalt in the Ross Sea, Antarctica: Micronutrient behavior,
810 absence of scavenging, and relationships with Zn, Cd, and P, Biogeosciences, 7, 4059-4082,
811 doi:10.5194/bg-7-4059-2010, 2010.

812 Saito, M. A., Noble, A. E., Hawco, N., Twining, B. S., Ohnemus, D. C., John, S. G., Lam, P.,
813 Conway, T. M., Johnson, R., Moran, D., and McIlvin, M.: The acceleration of dissolved
814 cobalt's ecological stoichiometry due to biological uptake, remineralization, and scavenging in
815 the Atlantic Ocean, Biogeosciences, 14, 4637-4662, doi:10.5194/bg-14-4637-2017, 2017.

816 Sarmiento, J. L., Gruber, N., Brzezinski, M. A., and Dunne, J. P.: High-latitude controls of
817 thermocline nutrients and low latitude biological productivity, Nature, 427, 56-60,
818 doi:10.1038/Nature02127, 2004.

819 Schlitzer, R., Anderson, R. F., Dodas, E. M., Lohan, M., Geibert, W., Tagliabue, A., et al.: The
820 GEOTRACES intermediate data product 2017, Chemical Geology, 493, 210-223, 2018.

821 Shaked, Y., Xu, Y., Leblanc, K., and Morel, F. M. M.: Zinc availability and alkaline
822 phosphatase activity in Emiliania huxleyi: Implications for Zn-P co-limitation in the ocean,
823 Limnol. Oceanogr., 51, 299-309, doi:10.4319/lo.2006.51.1.0299, 2006.

824 Sunda, W. G., and Huntsman, S. A.: Feedback interactions between zinc and phytoplankton in
825 seawater, Limnol. Oceanogr., 37, 25-40, doi:10.4319/lo.1992.37.1.0025 1992.

826 Sunda, W. G., and Huntsman, S. A.: Cobalt and zinc interreplacement in marine phytoplankton:
827 biological and geochemical implications, Limnol. Oceanogr., 40, 1404-1417,
828 doi:10.4319/lo.1995.40.8.1404, 1995.

829 Sunda, W. G., and Huntsman, S. A.: Control of Cd concentrations in a coastal diatom by
830 interactions among free ionic Cd, Zn, and Mn in seawater, Environ. Sci. Technol., 32, 2961-
831 2968, doi:10.1021/es980271y, 1998.

832 Sunda, W. G., and Huntsman, S. A.: Effect of Zn, Mn, and Fe on Cd accumulation in
833 phytoplankton: Implications for oceanic Cd cycling, Limnol. Oceanogr., 45, 1501-1516,
834 doi:10.4319/lo.2000.45.7.1501, 2000.

835 Tagliabue, A., Hawco, N. J., Bundy, R. M., Landing, W. M., Milne, A., Morton, P. L., and
836 Saito, M. A.: The role of external inputs and internal cycling in shaping the global ocean cobalt
837 distribution: insights from the first cobalt biogeochemical model, Global Biogeochem. Cy., 32,
838 594-616, doi:10.1002/2017gb005830, 2018.

839 Twining, B. S., and Baines, S. B.: The trace metal composition of marine phytoplankton, Annu.
840 Rev. Mar. Sci., 5, 191-215, doi:10.1146/annurev-marine-121211-172322, 2013.

841 Vance, D., Little, S. H., de Souza, G. F., Khatiwala, S., Lohan, M. C., and Middag, R.: Silicon
842 and zinc biogeochemical cycles coupled through the Southern Ocean, Nat. Geosci., 10, 202-
843 206, doi:10.1038/ngeo2890, 2017.

844 Weber, T., John, S., Tagliabue, A., and DeVries, T.: Biological uptake and reversible
845 scavenging of zinc in the global ocean, Science, 361, 72-76, doi:10.1126/science.aap8532,
846 2018.

847 Woodward, E. M. S., and Rees, A. P.: Nutrient distributions in an anticyclonic eddy in the
848 northeast Atlantic Ocean, with reference to nanomolar ammonium concentrations, Deep-Sea
849 Res. Pt II, 48, 775-793, doi:10.1016/S0967-0645(00)00097-7, 2001.

850 Wu, J. F., Sunda, W., Boyle, E. A., and Karl, D. M.: Phosphate depletion in the western North
851 Atlantic Ocean, Science, 289, 759-762, doi:10.1126/science.289.5480.759, 2000.

852 Wyatt, N. J., Milne, A., Woodward, E. M. S., Rees, A. P., Browning, T. J., Bouman, H. A.,
853 Worsfold, P. J., and Lohan, M. C.: Biogeochemical cycling of dissolved zinc along the
854 GEOTRACES South Atlantic transect GA10 at 40°S, Global Biogeochem. Cy., 28, 44-56,
855 doi:10.1002/2013gb004637, 2014.

856 Xu, Y., Tang, D., Shaked, Y., and Morel, F. M. M.: Zinc, cadmium, and cobalt
857 interreplacement and relative use efficiencies in the coccolithophore Emiliania huxleyi,
858 Limnol. Oceanogr., 52, 2294-2305, doi:10.4319/lo.2007.52.5.2294, 2007.

859 Zubkov, M. V., Fuchs, B. M., Tarran, G. A., Burkill, P. H., and Amann, R.: High rate of uptake
860 of organic nitrogen compounds by Prochlorococcus cyanobacteria as a key to their dominance
861 in oligotrophic oceanic waters, Appl. Environ. Microb., 69, 1299–1304,
862 doi:10.1128/aem.69.2.1299-1304.2003, 2003.

863

864

865

866 Table 1. Analytical validation results for open ocean surface seawater (SAFe S), 1000 m
867 seawater (SAFe D2) and 2000 m seawater (GEOTRACES GD). All concentrations are in nM
868 (± 1 std. dev.). Consensus value conversion = 1.025 kg/L. ND indicates sample not determined.

869

| | SAFe S | SAFe D2 | GEOTRACES GD |
|---|---|---|---|
| Zn (FIA) | 0.060 (0.020) *n* = 7 | 7.723 (0.091) *n* = 12 | ND |
| Zn consensus value | 0.071 (0.010) | 7.616 (0.256) | 1.753 (0.123) |
| Co (FIA) | 0.004 (0.001) *n* = 3 | 0.049 (0.001) *n* = 2 | 0.073 (0.004) *n* = 5 |
| Co consensus value | 0.005 (0.001) | 0.047 (0.003) | 0.067 (0.001) |

870

871

872 Table 2. Southeast Atlantic dissolved micro- and macronutrient mean concentration inventories
873 for the upper water column during early spring (D357-1), late spring (D357-2) and summer

(JC068) transects. STSW and SASW waters were defined using the θ 15°C isotherm (Section 3.4) and are compared with total inventories calculated for the shallower mixed layer (in parenthesis) that include continental inputs of dissolved Zn and Co. $Zn/PO_4^{3-}$, $Co/PO_4^{3-}$ and Zn/Co represent the concentration inventory ratios for STSW and SASW, respectively. STSW = Sub-Tropical Surface Water, SASW = Sub-Antarctic Surface Water.

| Oceanographic Regime | Transect | Zn (nmol $m^{-3}$) | Co (nmol $m^{-3}$) | $NO^{3-}$ (µmol $m^{-3}$) | $PO_4^{3-}$ (µmol $m^{-3}$) | $Si(OH)_4$ (µmol $m^{-3}$) | $Zn/PO_4^{3-}$ (µmol $mol^{-1}$) | $Co/PO_4^{3-}$ (µmol $mol^{-1}$) | Zn/Co (mol $mol^{-1}$) |
|---|---|---|---|---|---|---|---|---|---|
| STSW | Early spring | 624 (1597) | 32 (30) | 2694 (870) | 333 (203) | 3735 (2790) | 1876 | 97 | 19 |
| | Late spring | 384 (592) | 23 (17) | 1846 (763) | 276 (191) | 2781 (2326) | 1387 | 82 | 17 |
| | Summer | 158 (139) | 29 (24) | 1557 (326) | 226 (139) | 2711 (1942) | 699 | 129 | 5 |
| SASW | Early spring | 182 (112) | 14 (13) | 6035 (5300) | 615 (566) | 1875 (1847) | 296 | 22 | 13 |
| | Summer | 83 (94) | 12 (10) | 4143 (3388) | 439 (400) | 1027 (886) | 188 | 26 | 7 |

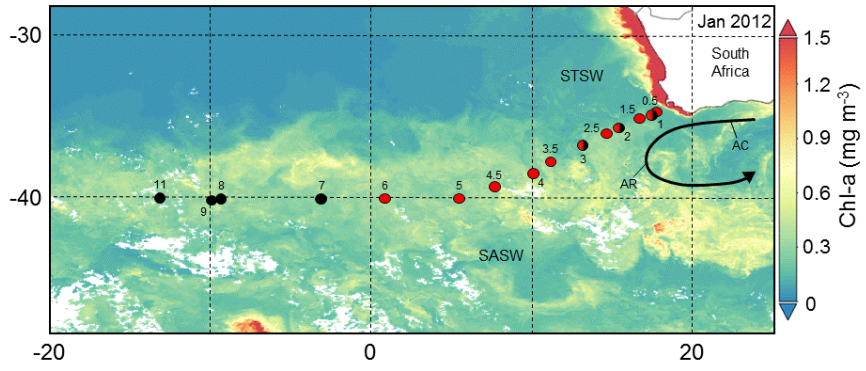


Figure 1. The Southeast Atlantic stations sampled for dissolved Zn and Co along the GA10 section during UK-GEOTRACES cruises D357 (red circles) and JC068 (black circles), overlain a VIIRS monthly composite image of chlorophyll-*a* concentrations for January 2012 (https://oceancolor.gsfc.nasa.gov/). Two transects were completed during D357 between Cape Town and the zero meridian that represent early austral spring 2010 (D357-1; Stns. 1, 2, 3, 4, 5 & 6) and late austral spring 2010 (D357-2; Stns. 0.5, 1, 1.5, 2.5, 3.5, 4.5), respectively. JC068 took place during austral summer 2011/12 and we present here only the repeat transect data

between Cape Town and 13°W (Stns. 1, 2, 3, 7, 8, 9, 11). STSW = Sub-Tropical Surface Water, SASW = Sub-Antarctic Surface Water, AC = Agulhas Current, AR = Agulhas retroflection.

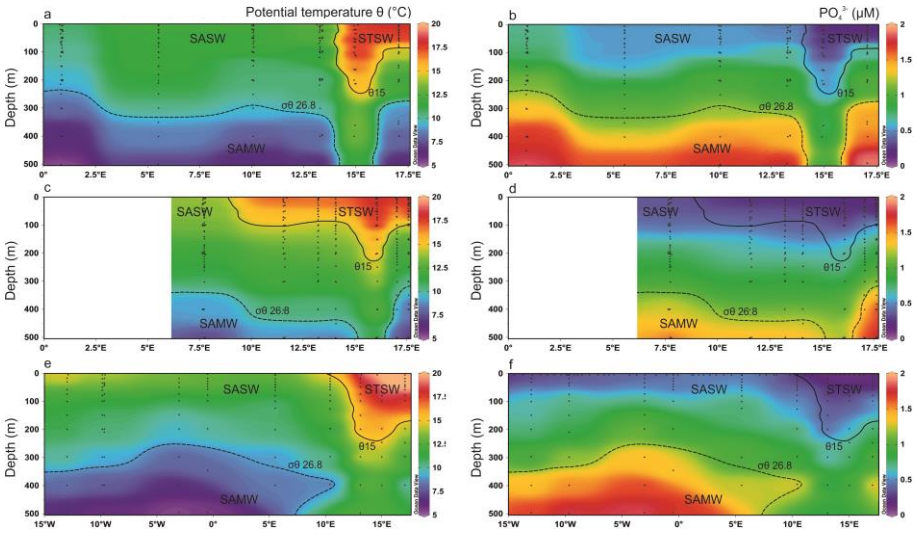


Figure 2. Upper 500 m potential temperature (θ) and dissolved $PO_4^{3-}$ distributions for the Southeast Atlantic along early spring (a,b; D357-1), late spring (c,d; D357-2) and summer (e,f; JC068) transects. The dominant Southern Ocean (SASW & SAMW) and South Atlantic (STSW) water masses that influence the distribution of nutrients are shown. The θ 15°C isotherm (solid contour) represents a practical definition of the STF location, whilst SAMW is identified by the median potential density (σθ) isopycnal 26.8 kg $m^{-3}$ (dashed contour, see Sect. 4.1.). STSW = Sub-Tropical Surface Water, SAMW = Sub-Antarctic Mode Water, AAIW = Antarctic Intermediate Water.

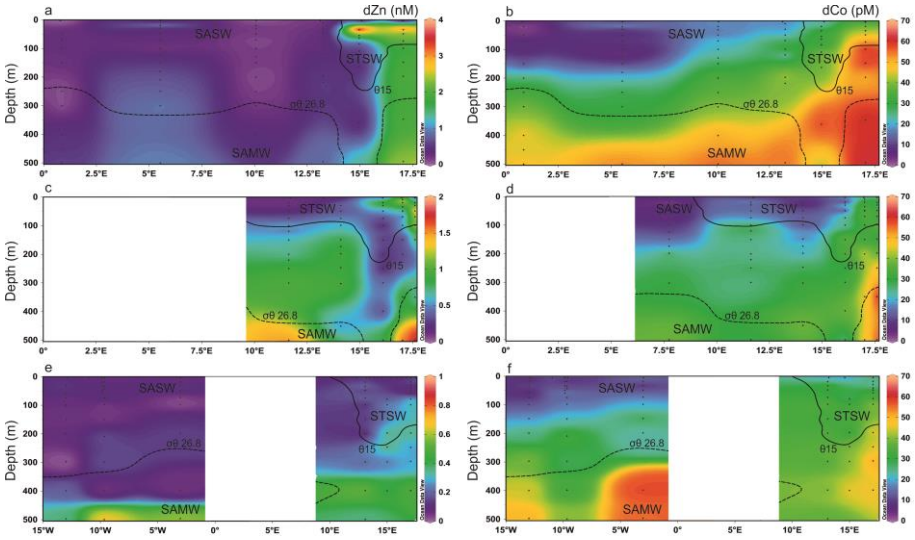


Figure 3. Upper 500 m dissolved Zn and Co distributions for the Southeast Atlantic along early spring (a,b; D357-1), late spring (c,d; D357-2) and summer (e,f; JC068) transects. The STF is delineated by θ 15°C (solid contour), whilst the influence of SAMW is evident by the median potential density (σθ) isopycnal 26.8 kg $m^{-3}$ (dashed contour, see Section 4.1.). STSW = Sub-Tropical Surface Water, SAMW = Sub-Antarctic Mode Water, AAIW = Antarctic Intermediate Water. Note the changing y-axis scales for dZn distribution.

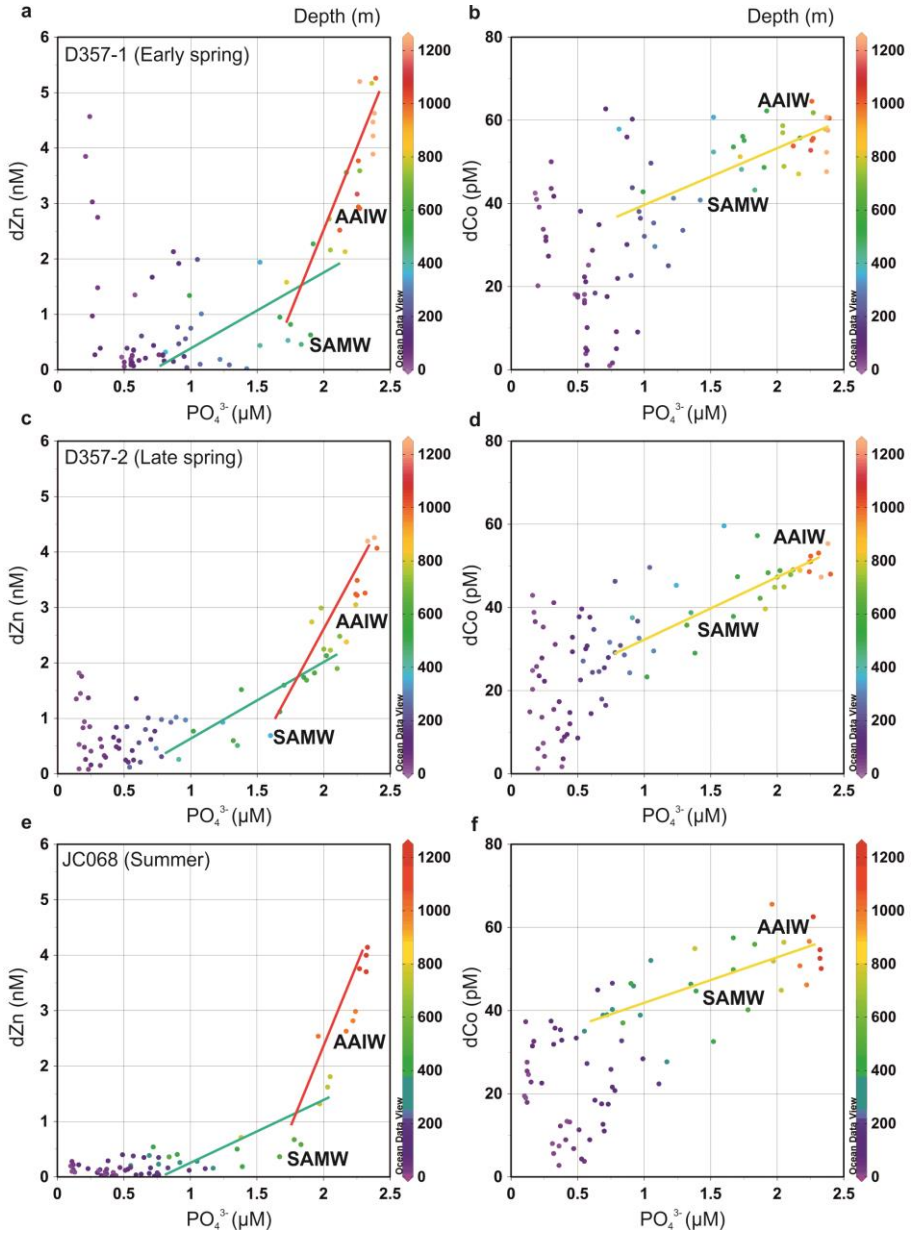


Figure 4. The dissolved Zn and Co versus $PO_4^{3-}$ distribution for the Southeast Atlantic during early spring (a,b; D357-1), late spring (c,d; D357-2) and summer (e,f; JCO68) transects. The green and red lines indicate the dZn:$PO_4^{3-}$ regression slopes for SAMW and AAIW, respectively. The yellow line indicates the dCo:$PO_4^{3-}$ regression slope for SAMW and AAIW combined. The equations for regression lines are detailed in Supplementary table 1. SAMW =

Sub-Antarctic Mode Water, AAIW = Antarctic Intermediate Water. The full depth dZn:$PO_4^{3-}$ relationship along JC068 can be found in Wyatt et al. (2014).

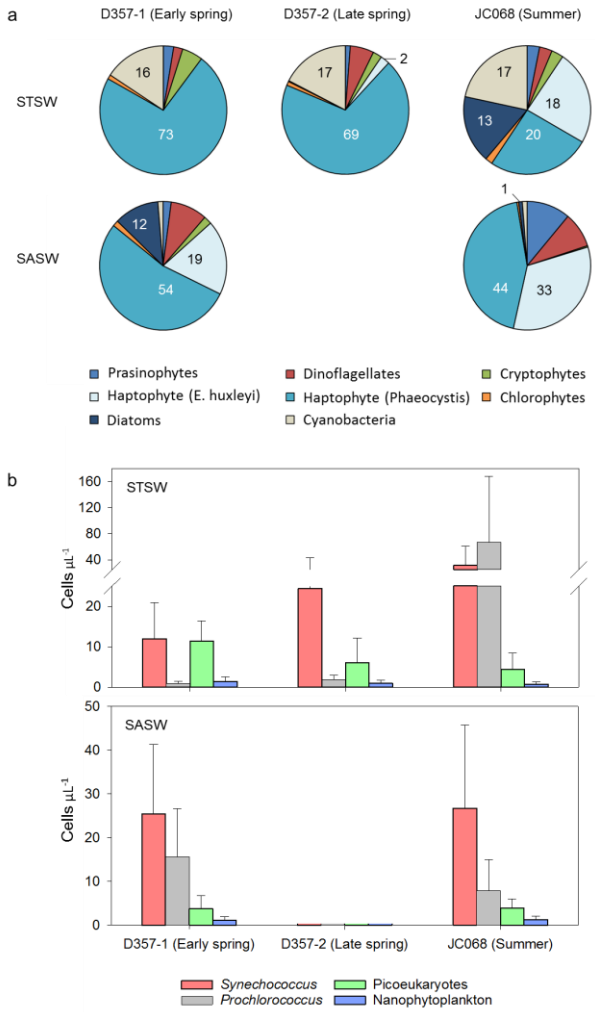


Figure 5. Seasonal differences in (a) pigment-derived taxonomic contributions to total chlorophyll-*a* (percentage), and (b) AFC counts of *Synechococcus*, *Prochlorococcus*, nanophytoplankton (approx. >2µm) and photosynthetic picoeukaryotes (approx. <2µm) in the Southeast Atlantic.

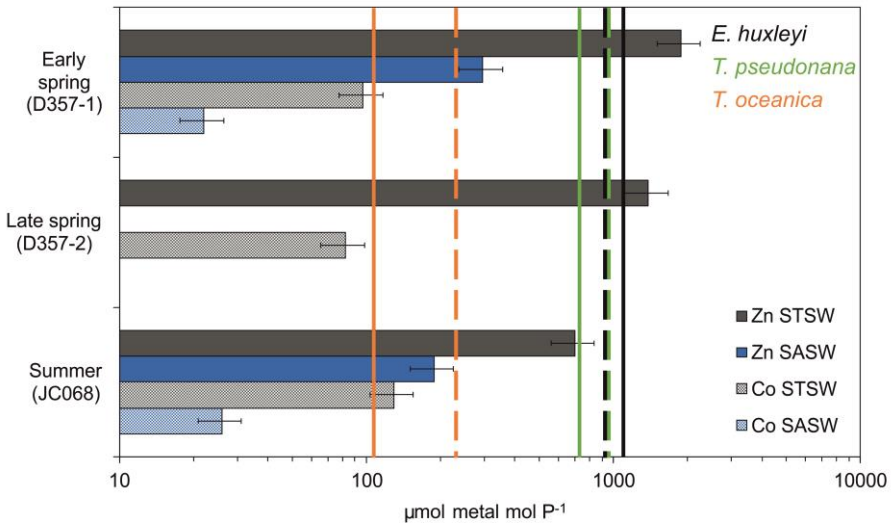


Figure 6. Metal/$PO_4^{3-}$ inventory ratios for the upper water column of the Southeast Atlantic (horizontal bars) compared with laboratory estimates of cellular ratios in eukaryotic phytoplankton below which growth limitation occurs (solid vertical lines represent Zn:P with no added Co to media whilst dashed lines represent Co:P with no added Zn; phytoplankton data from Sunda and Hunstman, 1995). Error bars on inventory ratios represent 20 % combined uncertainty for dZn and dCo analyses (see Section 2.2). This figure is adapted from that in Saito et al. (2010) and implies that inter-seasonal differences in metal/$PO_4^{3-}$ stoichiometry could impact phytoplankton community composition in the Southeast Atlantic.